Supporting Information

A self-assembled nanozyme featuring precise active centers and topography exhibits controlled catalytic interplay with mitochondrial protein while regulating electron flow during bioinspired oxygen reduction

Adarsh P. Fatrekar,[a,b] and Amit A. Vernekar*[a,b]

a A. P. Fatrekar, Dr. A. A. Vernekar
Inorganic and Physical Chemistry Laboratory
CSIR-Central Leather Research Institute (CLRI)
Adyar, Chennai-600020, India
E-mail: amitvernekar@clri.res.in

b A. P. Fatrekar, Dr. A. A. Vernekar
Academy of Scientific and Innovative Research (AcSIR)
Ghaziabad-201002, India

Table of Contents

Chemicals

Catalase from bovine liver, superoxide dismutase (SOD) bovine, terephthalic acid, sodium chloride, coumarin 99%, hydrogen peroxide (H_2O_2) solution 30%, sodium hydroxide (NaOH), ampliflu red (amplex red) for fluorescence, 98%, were purchased from Sigma-Aldrich chemicals Pvt. Ltd. Sephadex G-25 coarse was purchased from Pharmacia fine chemicals AB, Uppsala, Sweden. Cytochrome c (cyt c) oxidized type 1 ex. horse heart extrapure, horseradish peroxidase (HRP), L-phenylalanine extrapure, 99%, cupric chloride pure 98%, urea extrapure, 3,3',5,5'-tetramethylbenzidine dihydrochloride anhydrous, 99% (TMB), acetone extrapure, 99.5%, L-tryptophan, sodium phosphate dibasic anhydrous, 99%, sodium phosphate monobasic monohydrate, 99%, and nickel (II) chloride hexahydrate were purchased from SRL Chemicals Pvt. Ltd. Cobalt (II) chloride hexahydrate, sodium dithionite was purchased from S. D. fine-chem limited.

Characterization

UV-visible spectra were analyzed on Shimadzu UV-1800 UV spectrophotometer, scanning electron microscopy (SEM) imaging and X-ray mapping was performed using TESCAN, CLARA scanning electron microscope. FTIR and ATR-FTIR were recorded on Jasco FTIR-4700. Powder XRD analysis was performed on the Rigaku mini flex-II desktop (Cu Kα 1.5406 Å radiation). X-ray photoelectron spectroscopy (XPS) was recorded on a Thermo Scientific, MultiLab 2000 with Al Kα radiation (1486.6 eV) operated at 15 KV. Circular dichroism (CD) spectra were recorded on the Jasco J-815 CD spectrometer. The Zeta potential was measured using Malvern ZETASIZER Nano Series (ZEN3600 model) instrument.

1. Synthesis of copper-phenylalanine (Cu-Phen)

Cu-Phen was synthesized by following a previously reported procedure.[1] 500 mL, 5 mM $CuCl_2$ solution prepared in distilled water and 500 mL, 10 mM L-phenylalanine solution in 10 mM NaOH were heated at 60 ^oC. $CuCl_2$ solution was slowly added to L-phenylalanine solution at 60 ^oC. The heating was stopped after 10 min and the resultant solution was filtered after cooling. The filtered compound was washed four times with distilled water and once with ethanol and was dried in an oven at 60 ^oC.

2. Reduction and purification of cyt c

Sephadex G-25 beads were soaked overnight in phosphate buffer (50 mM pH 7.4) and were packed in a column. 2 mg ferric cyt c was dissolved in 120 µL phosphate buffer and was reduced by adding excess (approximately 20 mg) solid sodium dithionite. This reduced cyt c was eluted from the Sephadex column by using phosphate buffer as an eluent. The Sephadex column was washed with phosphate buffer till it was free from sodium dithionite and was used for subsequent elution. The concentration of eluted reduced cyt c was calculated by measuring its absorbance at 550 nm. The molar extinction coefficient of ferrous cyt c at 550 nm is 27.6 mM^{-1} cm^{-1}.

3. Studying electron transfer through Cyt c oxidase (CcO)-like activity

To the 10 µM solution of ferrous cyt c in phosphate buffer (50 mM pH 7.4), 10 µg mL^{-1} Cu-Phen was added. The solution was immediately mixed and its absorbance spectra were recorded. For time-dependent kinetics, the decrease in the absorbance of this reaction was monitored at 550 nm. A control reaction was performed without the addition of Cu-Phen.

4. Effect of free Cu^{2+} ions and leaching of Cu^{2+} on the electron transfer activity of Cu-Phen

To understand if the leaching of Cu^{2+} ions, if any, has a role in the CcO-like activity of Cu-Phen, the supernatant obtained after centrifugation of Cu-Phen incubated buffer was used for determining the activity. The activity assay followed was similar to the one discussed above. The initial rate of this reaction was calculated to understand if Cu^{2+} ions were leached to show any activity. In another experiment, the activity was carried out using Cu^{2+} ions (equivalent concentration to Cu^{2+} in Cu-Phen used in the assay).

5. Effect of concentration of Cu-Phen on the CcO-like activity

The kinetics of CcO-like activity were studied by varying the concentration of Cu-Phen from 0-10 µg in the reaction mentioned above. From the activity plots, the initial rates were calculated and plotted against Cu-Phen concentration.

6. Michaelis Menten Kinetics

The Michaelis Menten kinetics of CcO-like activity of Cu-Phen was performed by varying cyt c concentration from 2.5-20 µM in the reaction mentioned above. From the activity plots, the initial rates were calculated and plotted against the concentration of cyt c. The plot was fitted using

the Michaelis Menten curve fit. The Lineweaver-Burk plot was obtained by plotting 1/V versus 1/cyt c concentration, which could be fitted to a straight line. Kinetic parameters such as V_{max}, K_M and K_{cat}/K_M were calculated from the Lineweaver-Burk plot.

7. CD spectroscopy of cyt c

50 µg mL^{-1} Cu-Phen was reacted with 50 µM ferrous and ferric cyt c in phosphate buffer (20 mM pH 7.4) and CD spectra of these reactions were recorded from 190 – 300 nm and 300 – 500 nm after 10 min. CD spectra of 50 µM ferrous and ferric cyt c in phosphate buffer (20 mM pH 7.4) after 10 min were recorded as control.

8. Effect of pH on the CcO-like activity of Cu-Phen

The effect of pH on the CcO-like activity of Cu-Phen was evaluated by varying the pH from 6-8 in the reaction mentioned above. From the activity plots, the initial rates were calculated to understand the effect of pH.

9. CcO-like activity of Cu-phen in presence of urea, NaCl and dimethyl sulfoxide (DMSO)

10 µM phosphate buffered (50 mM pH 7.4) solution of ferrous cyt c was prepared in 0.5 M urea or 0.5 M NaCl or 10 % DMSO and to it 10 µg mL^{-1} Cu-Phen was added. The reaction mixtures were immediately mixed and the decrease in absorbance was recorded at 550 nm in a time-dependent manner. The control reaction was performed without the addition of urea, NaCl or DMSO. From the plots of time versus absorbance, the rates of the reactions were calculated.

8. CcO-like activity of Cu-Phen under O_2-deprived conditions

10 µg Cu-Phen was added to an N_2 purged solution of 10 µM ferrous cyt c in phosphate buffer (50 mM pH 7.4). The solution was immediately mixed and the decrease in absorbance was recorded at 550 nm in a time-dependent manner. The initial rates calculated for this reaction were compared with the control experimental reaction, which was performed without purging N_2.

10. CcO-like activity of Cu-Phen in the presence of SOD and Catalase

To the 10 µM solution of ferrous cyt c in phosphate buffer (50 mM pH 7.4), 10 µg mL^{-1} Cu-Phen and 1 U SOD or 1 U catalase was added. The solutions were immediately mixed and the decrease in absorbance were recorded at 550 nm in a time-dependent manner. The control reactions were performed without the addition of SOD and catalase.

11. H_2O_2 detection using ampliflu (amplex) red

10 μM ferrous cyt c was reacted with 10 μg mL^{-1} Cu-Phen in phosphate buffer (50 mM pH 7.4) in the presence of 5 units HRP and 10 μM ampliflu red. The fluorescence spectrum of this reaction was recorded after 30 min. Similarly, the fluorescence spectra of controls (10 μM ferrous cyt c + 5 units HRP + 10 μM ampliflu red; and 10 μM ampliflu red + 5 units HRP + 0.5 μM H_2O_2) were also recorded after 30 min.

12. Hydroxyl radical detection using terephthalic acid

15 μM ferrous cyt c was reacted with 10 μg mL^{-1} Cu-Phen in phosphate buffer (50 mM pH 7.4) in the presence of 0.5 mM terephthalic acid solution. The fluorescence spectrum of this reaction was recorded after 30 min by exciting at 315 nm. Similarly, the fluorescence spectra of controls (15 μM ferrous cyt c + 0.5 mM terephthalic acid; 10 μg mL^{-1} Cu-Phen + 0.5 mM terephthalic acid; and 0.5 mM terephthalic acid) were also recorded after 30 min.

13. Kinetic isotope effect on the electron transfer from cyt c to Cu-Phen in deuterated buffer

The decrease in absorbance at 550 nm of the reaction mixture containing 10 μM cyt c, 10 μg mL^{-1} Cu-Phen in 50 mM phosphate buffer (pH 7.4, pD 7.81) prepared in D_2O was studied in a time-dependent manner. The initial rate obtained was compared with the experimental control reaction performed in 50 mM phosphate buffer (pH 7.4). The rate constants (calculated using a first-order equation) were calculated to determine the ratio K_H/K_D to understand the kinetic isotope effect.

Note: 45 μM ferrous cyt c stock was prepared in 50 mM phosphate buffer (pH 7.4) and used in the above assay.

14. Recyclability of Cu-Phen for CcO activity

0.5 mg Cu-Phen was dispersed in a 10 μM solution of ferrous cyt c in phosphate buffer (50 mM pH 7.4) and its decrease in absorbance was monitored at 550 nm. After the reaction, the solution was centrifuged at 13000 rpm for 5 min to isolate Cu-Phen. The supernatant was discarded and to the isolated Cu-Phen, fresh 10 μM ferrous cyt c solution was added and its decrease in absorbance was monitored at 550 nm. The process was repeated for five more cycles and the rates of each cycle were compared.

15. Superoxide scavenging activity of Cu-Phen

0.5 mM xanthine was reacted with 33 mU xanthine oxidase (XO) in the presence of 2 µL WST-1 and 50 µg mL^{-1} Cu-Phen for 10 min in phosphate buffer (50 mM pH 7.4) and its absorbance spectrum was recorded. The same reaction without the addition of Cu-Phen was performed as a control and its absorbance spectrum was recorded after 10 min. The reaction of WST-1 with superoxide produces the corresponding formazan that absorbs at 440 nm. No formation of formazan indicates superoxide scavenging of Cu-Phen that scavenges generated superoxide.

16. Protein and self-assembly images

The images of proteins, cyt c, CcO, HRP and XO, were created using Chimera software and PDB entries 1OCD, 5Z62, 1HCH, and 1FIQ, respectively. The design of Cu-Phen was created using the previously reported X-ray crystallographic coordinates of Cu-Phen (accession code 1871975 in the Cambridge Crystallographic Data Centre (CCDC) database).[1]

Note: For proper visualization of plots, the time-dependent monitoring of cyt c oxidation has been normalized to a constant initial absorbance. The upward protrusion due to the increase in absorbance as observed in some time-dependent absorbance plots is probably due to the changes in the differential scattering of light by the dispersed Cu-Phen sheets (particles) of various sizes, when they appear in the path of the light.

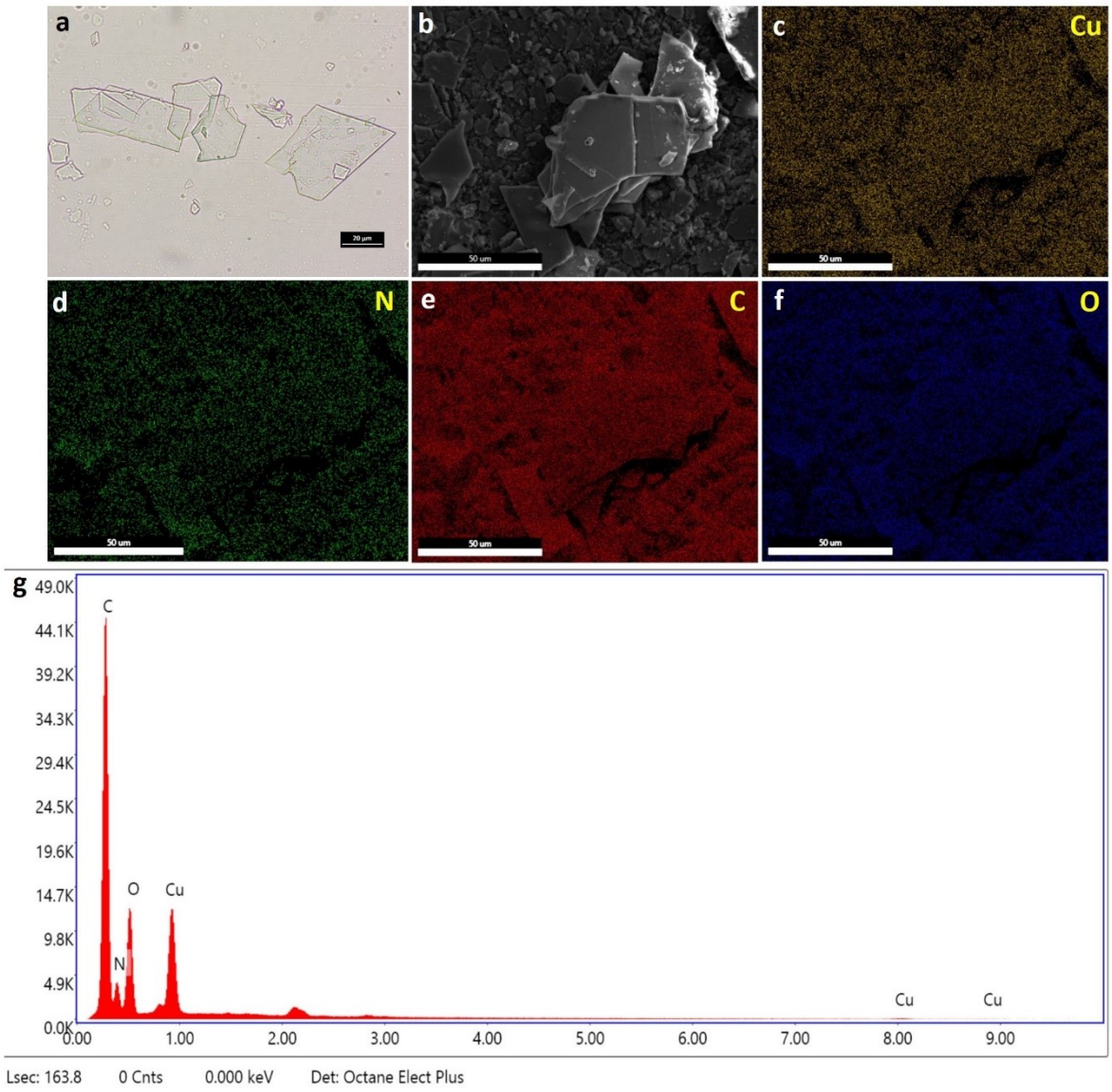

Figure S1. a) Optical microscope image of Cu-Phen; **b)** SEM image of Cu-Phen showing the area used for elemental X-ray mapping of; **c-f)** Cu, N, C and, O; **g)** EDX spectrum of Cu-Phen.

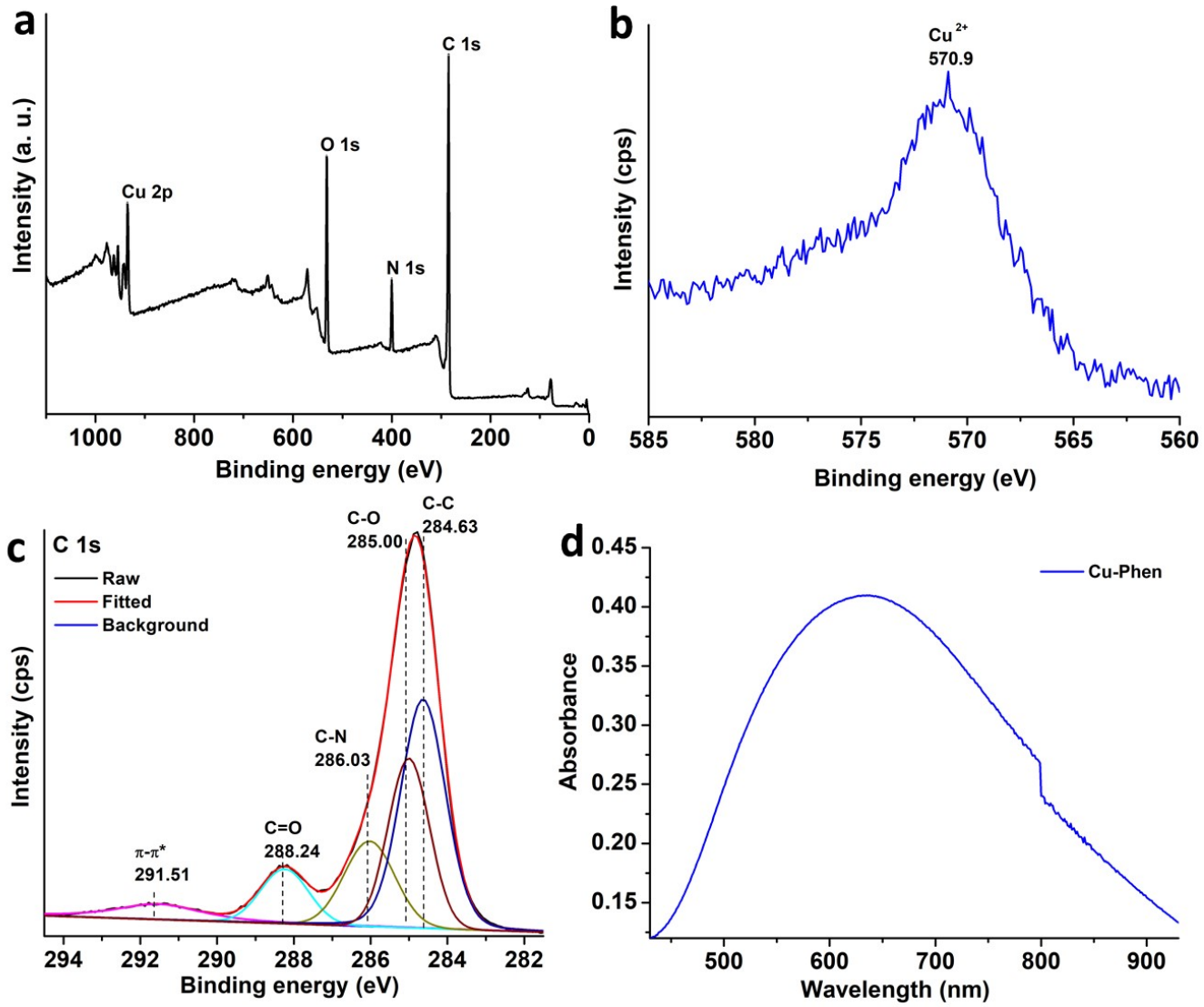

Figure S2. a) Survey XPS spectrum of Cu-Phen; **b)** Cu-LMM spectrum; **c)** C1s XPS spectra of Cu-Phen; **d)** Solid state UV-DRS spectrum of Cu-Phen.

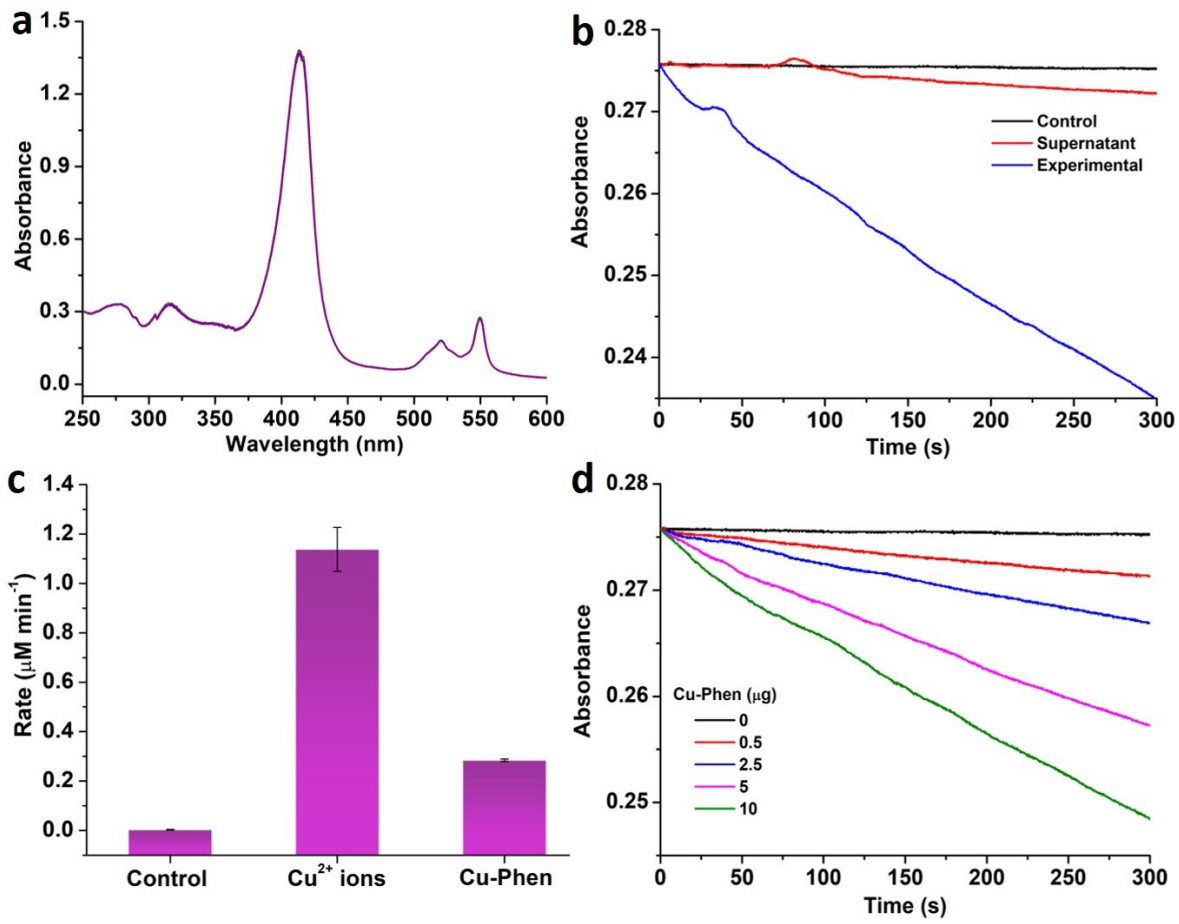

Figure S3. a) UV-visible spectra showing the oxidation of ferrous cyt c without Cu-Phen; **b)** Time-dependent absorbance spectra for the CcO-like activity of control cyt c, Cu-Phen supernatant obtained after centrifugation and experimental; **c)** Comparison of CcO-like activities of free Cu^{2+} ions, Cu-Phen, and control. **d)** Time-dependent absorbance spectra for the CcO-like activity in the presence of different amounts of Cu-Phen.

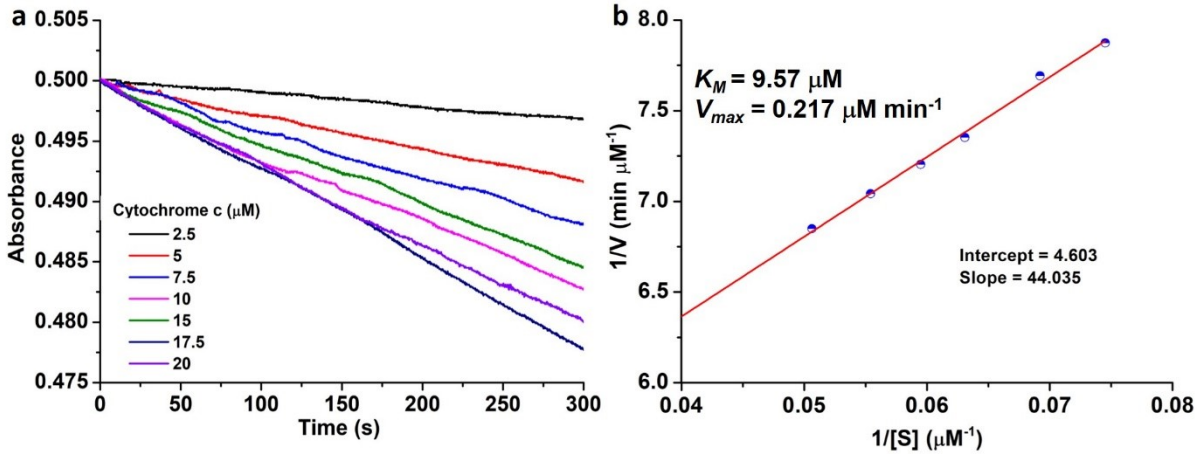

Figure S4. a) Time-dependent absorbance spectra for the CcO-like activity of Cu-Phen at different concentrations of cyt c; **b)** Lineweaver-Burk plot obtained by plotting 1/V versus 1/cyt c concentration.

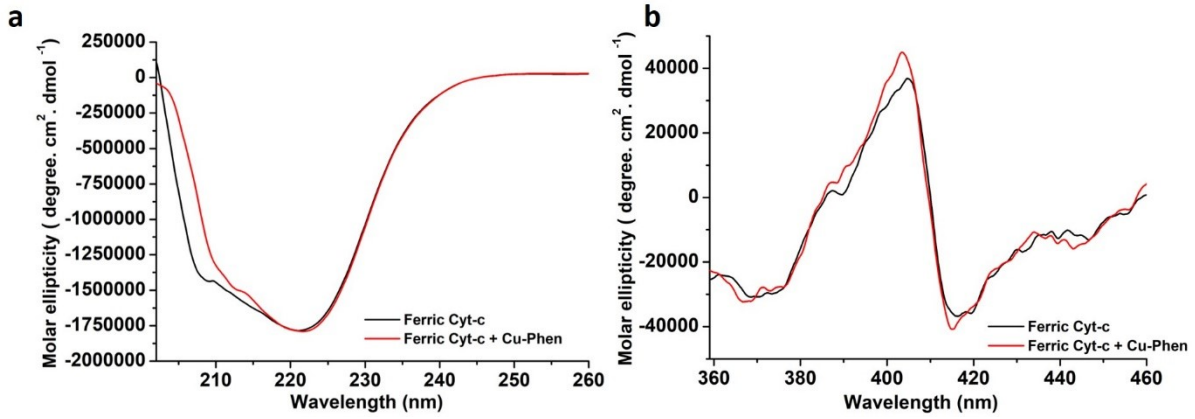

Figure S5. a,b) CD spectra of ferric cyt c showing its interaction with Cu-Phen.

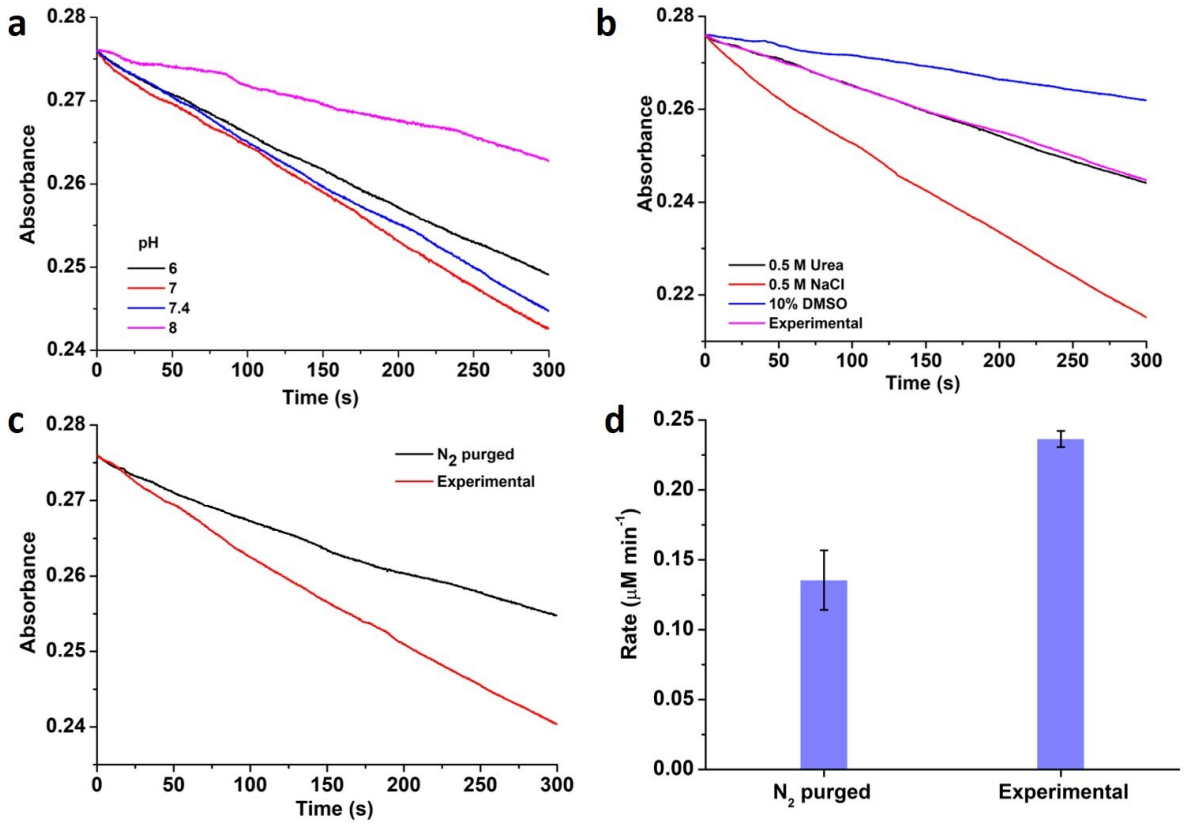

Figure S6. Time-dependent absorbance spectra for the CcO-like activity of Cu-Phen, **a)** Under different physiologically relevant pH; **b)** In the presence of urea, NaCl, DMSO; **c)** Under oxygen-deprived condition; **d)** Initial rate for the CcO-like activity of Cu-Phen under oxygen-deprived condition.

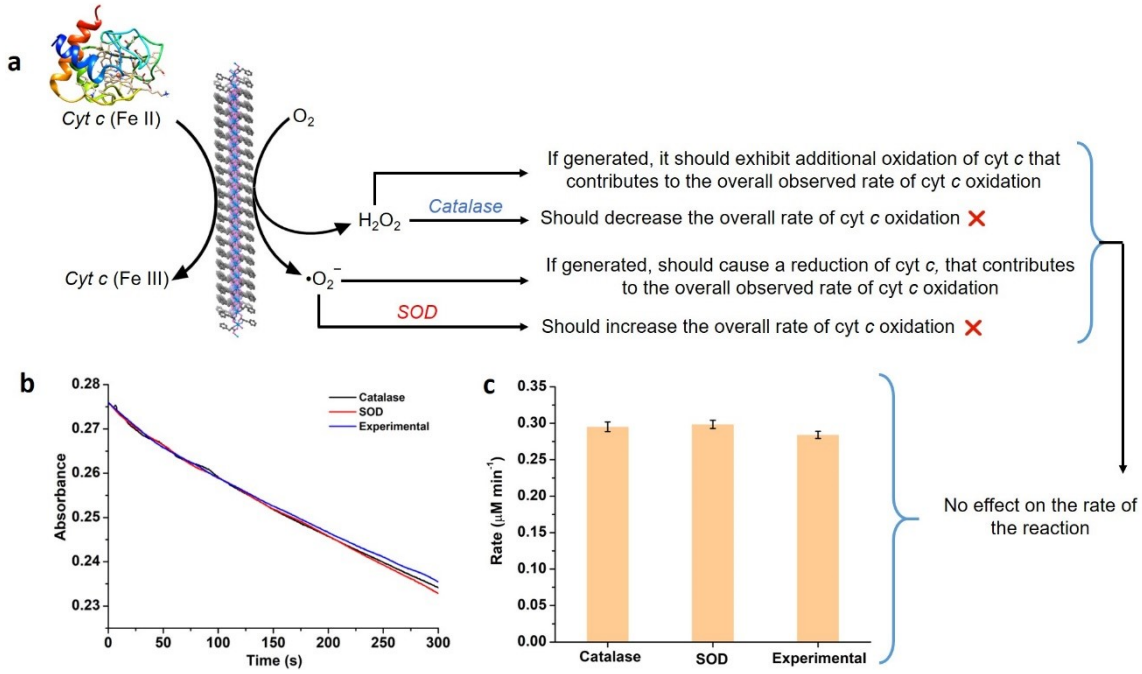

Figure S7. a) Scheme showing the possible production of PROS such as H_2O_2 or superoxide radical during the CcO-like activity of Cu-Phen; **b,c)** Time-dependent absorbance spectra and initial rates of the reactions for the CcO-like activity of Cu-Phen in presence of catalase, and SOD enzymes.

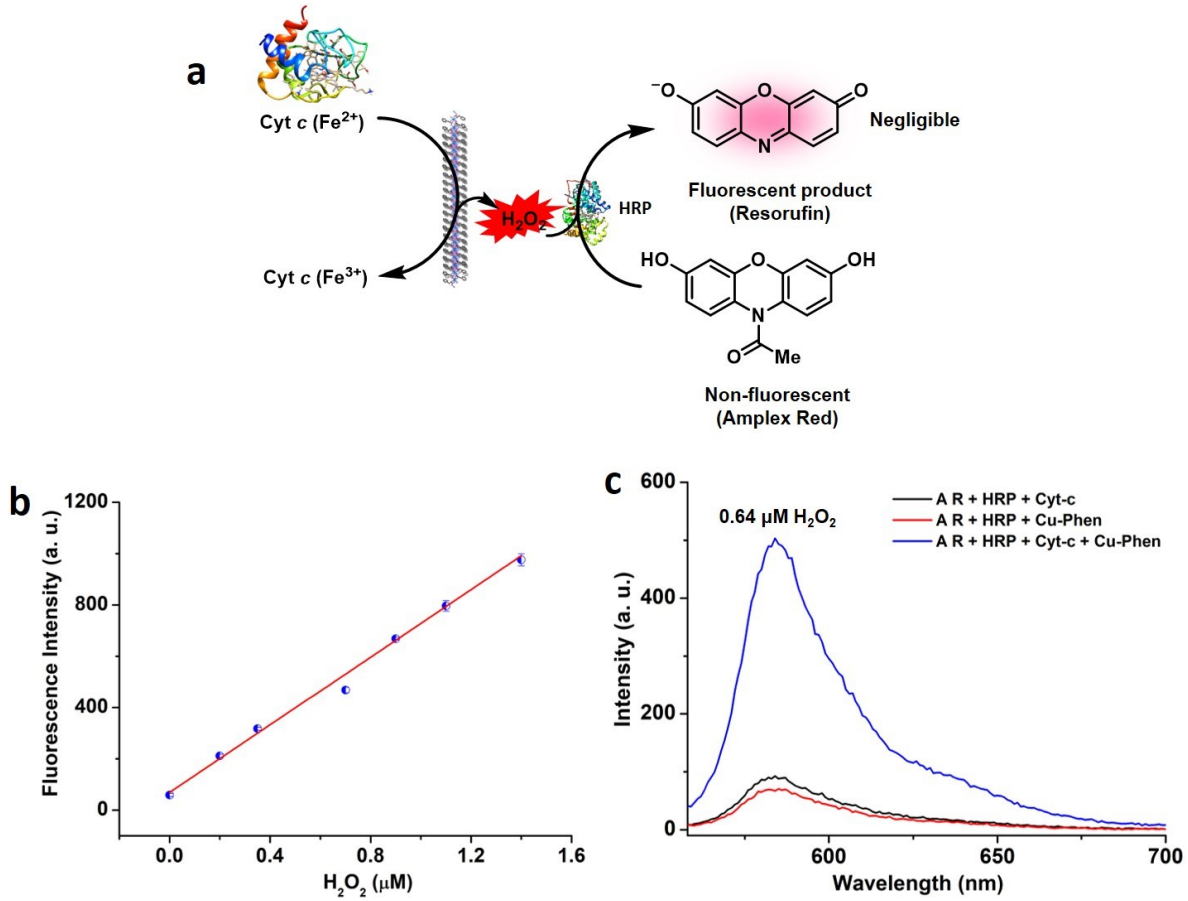

Figure S8. a) Scheme showing the production of H_2O_2 during the CcO-like activity of Cu-Phen, and its detection by amplex red; **b)** Calibration curve for finding the concentration of H_2O_2 produced during the CcO-like activity of Cu-Phen; **c)** Fluorescence spectra for detection of H_2O_2 using amplex red assay.

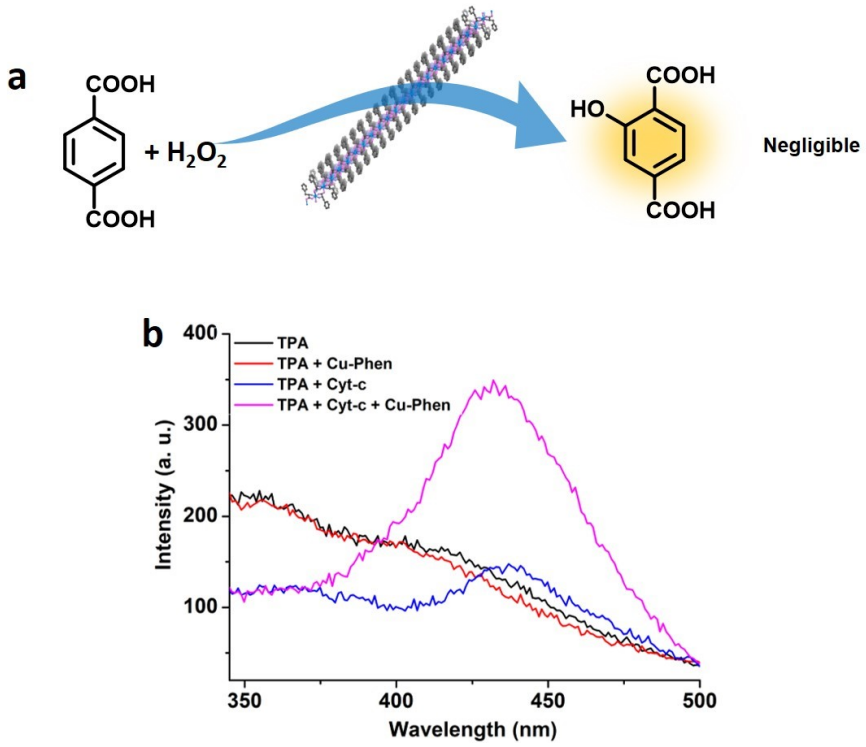

Figure S9. a) Scheme showing the reaction of terephthalic acid with the hydroxyl radical generated during the CcO-like activity of Cu-Phen to form fluorescent product, hydroxy terephthalic acid; **b)** Fluorescence spectra showing the formation of hydroxy terephthalic acid during the CcO-like activity of Cu-Phen.

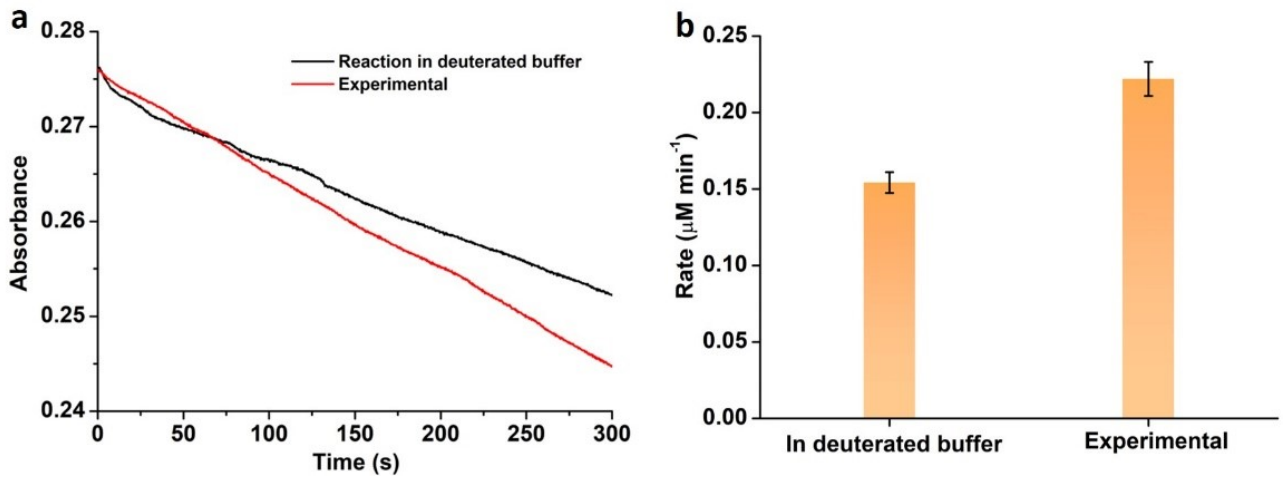

Figure S10. a) Time-dependent absorbance spectra for the CcO-like activity of Cu-Phen in the deuterated buffer; **b)** Comparison of rates of CcO-like activity under deuterated and non-deuterated buffer (experimental) conditions.

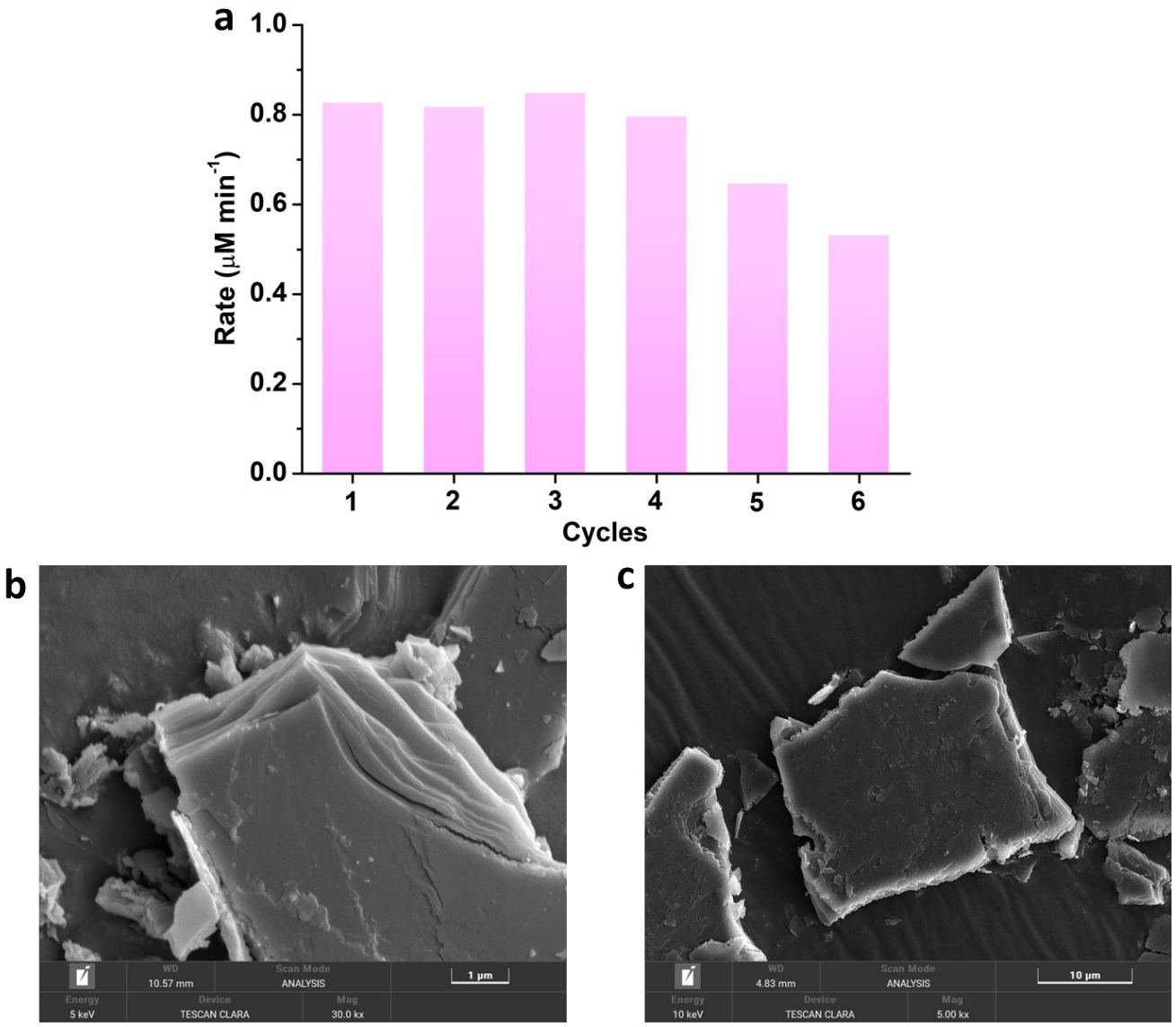

Figure S11. a) Plot showing the initial rates of reactions for the recyclability experiment of CcO-like activity of Cu-Phen; **b-c)** SEM images of Cu-Phen obtained after testing recyclability.

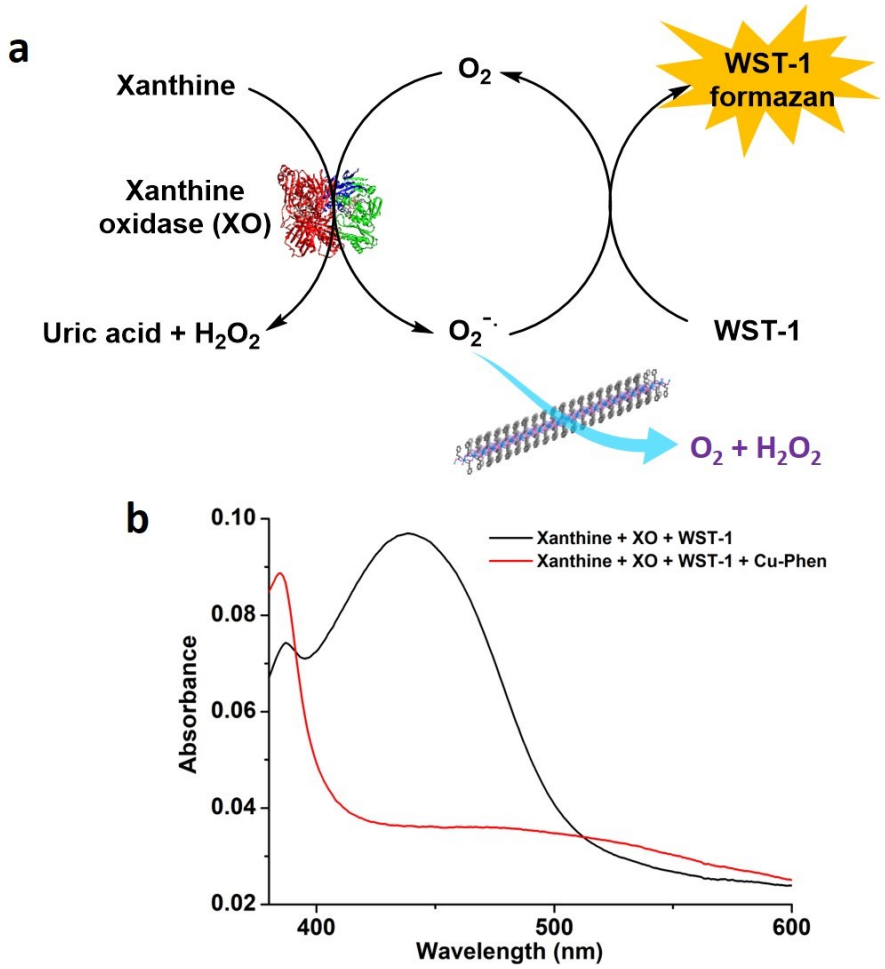

Figure S12. a) Scheme showing the assay conditions used for monitoring superoxide scavenging activity of Cu-Phen; **b)** Absorbance spectra showing the production of WST-1 formazan upon reaction with superoxide radical, and inhibition of WST-1 formazan production due to superoxide scavenging activity of Cu-phen.

References

1. Makam, P.; Yamijala, S. S. R. K. C.; Bhadram, V. S.; Shimon, L. J. W.; Wong, B. M.; Gazit, E. Single Amino Acid Bionanozyme for Environmental Remediation. *Nat. Commun.,* 2022, **13**, 1505.